Histochemistry and Cell Biology (2022) 157:239–250
https://doi.org/10.1007/s00418-021-02048-y

ORIGINAL PAPER

The bioavailability time of commonly used thymidine analogues after intraperitoneal delivery in mice: labeling kinetics in vivo and clearance from blood serum

Dmitry I. Maltsev[1,2] · Kennelia A. Mellanson[3] · Vsevolod V. Belousov[1,2,5] · Grigori N. Enikolopov[4,6] · Oleg V. Podgorny[2,5,7]

Accepted: 28 October 2021 / Published online: 10 November 2021
© The Author(s), under exclusive licence to Springer-Verlag GmbH Germany, part of Springer Nature 2021

Abstract

Detection of synthetic thymidine analogues after their incorporation into replicating DNA during the S-phase of the cell cycle is a widely exploited methodology for evaluating proliferative activity, tracing dividing and post-mitotic cells, and determining cell-cycle parameters both in vitro and in vivo. To produce valid quantitative readouts for in vivo experiments with single intraperitoneal delivery of a particular nucleotide, it is necessary to determine the time interval during which a synthetic thymidine analogue can be incorporated into newly synthesized DNA, and the time by which the nucleotide is cleared from the blood serum. To date, using a variety of methods, only the bioavailability time of tritiated thymidine and 5-bromo-2′-deoxyuridine (BrdU) have been evaluated. Recent advances in double- and triple-S-phase labeling using 5-iodo-2′-deoxyuridine (IdU), 5-chloro-2′-deoxyuridine (CldU), and 5-ethynyl-2′-deoxyuridine (EdU) have raised the question of the bioavailability time of these modified nucleotides. Here, we examined their labeling kinetics in vivo and evaluated label clearance from blood serum after single intraperitoneal delivery to mice at doses equimolar to the saturation dose of BrdU (150 mg/kg). We found that under these conditions, all the examined thymidine analogues exhibit similar labeling kinetics and clearance rates from the blood serum. Our results indicate that all thymidine analogues delivered at the indicated doses have similar bioavailability times (approximately 1 h). Our findings are significant for the practical use of multiple S-phase labeling with any combinations of BrdU, IdU, CldU, and EdU and for obtaining valid labeling readouts.

Keywords Thymidine analogues · Proliferation · BrdU (5-bromo-2′-deoxyuridine) · IdU (5-iodo-2′-deoxyuridine) · CldU (5-chloro-2′-deoxyuridine) · EdU (5-ethynyl-2′-deoxyuridine) · Immunohistochemistry · Click chemistry

Introduction

Tritiated thymidine and synthetic thymidine analogues are widely employed for marking replicating DNA during the S-phase of the cell cycle. Detection of these modified nucleotides after their incorporation into newly synthesized DNA enables examination of the spatial and temporal features of the DNA synthesis in the cell (Manders et al. 1996; Ma et al. 1998), the determination of cell cycle parameters (Nowakowski et al. 1989; Cai et al. 1997; Brandt et al. 2012), the evaluation of kinetics and modes of cell division (Takahashi et al. 1994; Alexiades and Cepko

✉ Oleg V. Podgorny
olegpodgorny@inbox.ru

1 Federal Center of Brain Research and Neurotechnologies, Federal Medical Biological Agency, Moscow, Russia 117997

2 Shemyakin-Ovchinnikov Institute of Bioorganic Chemistry, Russian Academy of Sciences, Moscow, Russia 117997

3 Molecular and Cellular Pharmacology Graduate Program and Center for Developmental Genetics, Stony Brook University, Stony Brook, NY 11794, USA

4 Center for Developmental Genetics and Department of Anesthesiology, Stony Brook University, Stony Brook, NY 11794, USA

5 Center for Precision Genome Editing and Genetic Technologies for Biomedicine, Pirogov Russian National Research Medical University, Moscow, Russia 117997

6 Institute for Advanced Brain Studies, Lomonosov Moscow State University, Moscow, Russia 119991

7 Koltzov Institute of Developmental Biology, Russian Academy of Sciences, Moscow, Russia 119334

1996; Hayes and Nowakowski 2000; Mandyam et al. 2007; Podgorny et al. 2018), cell birth dating (Angevine and Sidman 1961), and tracing the fate and migration of proliferating and postmitotic cells (Schweyer et al. 2019). The labeling of replicating DNA with modified nucleotides has become an indispensable method in cell biology, developmental biology, stem cell research, and cancer research and is used in both experiments on cultured cells in vitro and studies on various species in vivo.

The modified nucleotides used for cell cycle analysis can be subdivided into several groups: halogenated thymidine analogues that are detected by antibodies (Gratzner 1982; Vega and Peterson 2005), synthetic thymidine analogues that are detected by click chemistry reactions (Salic and Mitchison 2008; Neef and Luedtke 2011, 2014; Rieder and Luedtke 2014), and tritiated or stable isotope-labeled thymidine that is detected by autoradiography or multi-isotope mass-spectrometry imaging, respectively (Taylor et al. 1957; Steinhauser et al. 2012). To label newly synthesized DNA, cultured cells or organisms undergo treatment with modified nucleotides, usually via addition into the cell culture medium, ambient water (in the case of water inhabitants), or drinking water (in the case of terrestrial vertebrate species), or via intraperitoneal, intravenous, or intramuscular injections (applicable for most vertebrate species). Pulse-chase labeling and cumulative labeling are major DNA labeling schemes used in most studies. Combined with quantitative analysis of cells that have incorporated a particular label into their newly synthesized DNA, these labeling schemes enable various aspects of cell proliferation in diverse in vitro and in vivo systems to be revealed. Development of methods for discrimination between two or three distinct modified nucleotides led to creating double- and triple-S-phase labeling schemes for proliferating cells (Hayes and Nowakowski 2000; Vega and Peterson 2005; Rieder and Luedtke 2014; Podgorny et al. 2018). Temporal discrimination of two or three labels in combination with quantitative analysis increases the resolution of cell-cycle kinetics analysis and allows for multiple birth dating (Takahashi et al. 1993, 1994; Verdoodt et al. 2012; Brandt et al. 2012; Podgorny et al. 2018; Newton et al. 2019).

When marking dividing cells in cell cultures, the time interval during which a label builds into replicating DNA can be easily controlled by washing the cells from the label. This ensures reproducible labeling results and, for multiple labeling, allows for avoidance of label overlap. Unlike cell cultures, for intraperitoneal, intravenous, or intramuscular injections in most vertebrate species, the time interval during which a label incorporates into replicating DNA cannot be controlled instrumentally; instead, it is defined by the rate of label propagation via the blood circulation system and the rate of label metabolization. The time interval in which the entire amount of the modified nucleotide is completely metabolized is referred to as the bioavailability time. This characteristic of label behavior is critically important when performing quantitative analysis of labeled cells and multiple labeling in in vivo systems. Ignoring this parameter can affect labeling results, quantitative readouts, and interpretation of the experimental data.

A number of studies have reported evaluations of the bioavailability time for tritiated thymidine and 5-bromo-2′-deoxyuridine (BrdU), which are the most frequently used modified nucleotides, in several animal species, and even in humans (Rubini et al. 1960; Kriss and Revesz 1962; Staroscik et al. 1964; Packard et al. 1973; Nowakowski and Rakic 1974; Stetson et al. 1985; Phuphanich and Levin 1985; Hayes and Nowakowski 2000; Mandyam et al. 2007; Barker et al. 2013; Matiašová et al. 2014). The bioavailability time was primarily evaluated by either assessment of label uptake into replicating DNA using autoradiographic analysis or scintillation detection (Rubini et al. 1960; Staroscik et al. 1964; Packard et al. 1973) or by measurement of label clearance from the blood serum using scintillation detection, high-performance liquid chromatography, or cell culture assay (Packard et al. 1973; Nowakowski and Rakic 1974; Stetson et al. 1985; Phuphanich and Levin 1985; Barker et al. 2013; Matiašová et al. 2014). Taken together, these studies indicate that, after a pulse delivery, the bulk of both tritiated thymidine and BrdU is incorporated into replicating DNA within 15–25 min and label uptake reaches saturation within 1–2 h. Assessment of label clearance reveals that both labels cannot be detected in the blood serum 1–2 h after a pulse delivery.

After delivery into an organism, BrdU undergoes rapid degradation with formation of bromouracil and bromide ion (Kriss and Revesz 1962). Only a fraction of delivered BrdU escapes degradation and builds into replicating DNA. Liver was identified as a major site where BrdU is degraded via dehalogenation (Kriss and Revesz 1962). Besides liver, blood serum enzymes degrade BrdU and 5-iodo-2′-deoxyuridine (IdU), yet another thymidine analogue used for marking replicating DNA, via dehalogenation and conversion into bromo- and iodouracil, respectively (Saffhill and Hume 1986). Notably, rates of biodegradation of these thymidine analogues by blood serum enzymes were found to be dissimilar. Besides BrdU and IdU, the halogenated thymidine analogue 5-chloro-2′-deoxyuridine (CldU) and the "clickable" thymidine analogue 5-ethynyl-2′-deoxyuridine (EdU) are commonly used to mark replicating DNA in model rodents (mice and rats). Moreover, we have recently reported triple-S-phase labeling of dividing stem cells in vivo using combinations of IdU, CldU, and EdU (Podgorny et al. 2018). Since rates of biodegradation of halogenated thymidine analogues were found to be dissimilar (Saffhill and Hume 1986) and the mechanisms of biodegradation of EdU are unknown, it can be hypothesized that, despite the structural similarity of these thymidine analogues, their bioavailability time may vary enough to produce inconsistent quantitative readouts

in case of multiple S-phase labeling. To make labeling with these modified nucleotides consistent and reproducible, it is important to know how they behave after a single pulse delivery. Therefore, we evaluated IdU, CldU, and EdU in terms of labeling kinetics in vivo and the time of their complete clearance from the blood serum, and compared them to BrdU. To this end, we analyzed the numbers of labeled cells in the hippocampal dentate gyrus (DG) of adult mice at different time points after a single intraperitoneal injection of a modified nucleotide and, in parallel, assessed blood sera collected from the same mice by cell culture assay (Barker et al. 2013).

Materials and methods

Animals

Experiments were conducted using 8–10-week-old C57BL/6 male mice. Mice were group housed (3–4 mice per cage) in the animal facility at Shemyakin-Ovchinnikov Institute of Bioorganic Chemistry. All experimental procedures were performed according to the European Convention for the Protection of Vertebrate Animals used for Experimental and other Scientific Purposes (1986, ETS 123) and approved by the Institutional Animal Care and Use Committee (protocol no. 281). Mice were housed in a temperature-controlled (22–24 °C) room with a 12 h light/dark cycle and had ad libitum access to food and water.

Experimental design and sample collection

Ninety-six mice received single intraperitoneal injections of one of four thymidine analogues dissolved in saline: BrdU (Sigma-Aldrich, #B5002) at a dose of 150 mg/kg with a final concentration of 7.5 mg/ml ($n = 24$), IdU (Sigma-Aldrich, #I7125) at a dose of 173 mg/kg with a final concentration of 2.47 mg/ml ($n = 24$), CldU (Sigma-Aldrich, #C6891) at a dose of 128 mg/kg with a final concentration of 6.4 mg/ml ($n = 24$), or EdU (Lumiprobe, #40540) at a dose of 123 mg/kg with a final concentration of 6.15 mg/ml ($n = 24$). Doses of IdU, CldU, and EdU were equimolar to the saturating dose of 150 mg/kg of BrdU determined earlier (Mandyam et al. 2007). Mice were deeply anesthetized by intraperitoneal injection of a mixture of tiletamine/zolazepam/xylazine at doses of 40/40/20 mg/kg at the following time points (four animals per time point): 10, 20, 30, 60, 120, or 240 min after injection of the thymidine analogue (Fig. 1). The anesthetized mice underwent a surgical procedure necessary for transcardial perfusion. Before a perfusion needle was inserted into the left ventricle of the heart, blood leaking from the incised right atrium into the open thoracic cavity was collected using a 1-ml syringe without a needle into a 1.5-ml microcentrifuge tube. The collected blood was allowed to clot at 4 °C for 3 h and centrifuged at 3000 g for 30 min. The isolated sera were stored at −80 °C until needed. After the blood sample was collected, transcardial perfusion was conducted as usual. Brains were washed from

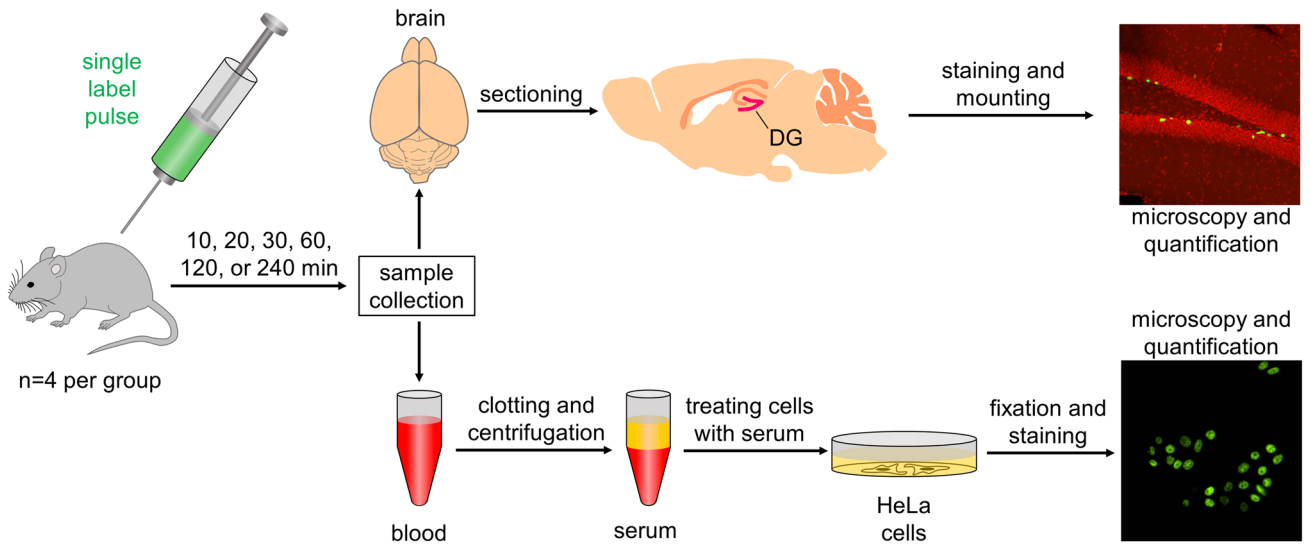

Fig. 1 The experimental design for examining the labeling kinetics of BrdU, IdU, CldU, and EdU in vivo and their clearance from the blood serum. Mice received a single intraperitoneal injection of a label and were deeply anesthetized at time points 10, 20, 30, 60, 120, and 240 min after label injection. Then, blood was collected, mice were transcardially perfused, and the brains were extracted. The brains were sliced and stained, and then labeled cells in the hippocampal DG were quantified using an epifluorescence microscope. The blood samples were left for clotting followed by centrifugation. HeLa cells were then treated for 30 min with isolated blood sera or pure labels at a concentration of 10 μM. Following the treatments, cells were fixed, stained, and imaged, and the images were used for determining the labeling indices and mean signal intensities

residual blood with prewarmed 0.01 M phosphate-buffered saline (PBS) (pH 7.4) followed by perfusion with ice-cold 4% paraformaldehyde in PBS (pH 7.4). Brains removed from the skulls were postfixed in 4% paraformaldehyde in PBS overnight at 4 °C.

Processing brain samples

Postfixed brains were washed with PBS, and the right hemispheres were sliced sagittally in a lateral-to-medial direction using a Leica VT1200S vibratome (Leica-Microsystems). The most lateral slices which do not contain the DG were discarded. When the DG became visible, we started to collect slices (thickness of 50 µm) into six wells of a 24-well plate filled with PBS according to a fractionator scheme as previously described (Encinas and Enikolopov 2008). The first slice was placed into the first well, the second slice was placed into the second well, and so on until the sixth was placed into the sixth well, then the seventh slice was placed into the first well, the eighth slice was placed into the second well, and so on until the hemisphere was completely sliced. Thus, each well contained a series of the 50-µm slices which were 250 µm apart. The series (10–11 slices) represented a fraction (one sixth) of the entire DG of one hemisphere.

Cultivation of HeLa cells and treatment with mouse blood sera

HeLa Kyoto cells were grown in Dulbecco's modified Eagle medium (Paneco) supplemented with 10% fetal bovine serum (PAA Laboratories), 2 mM L-glutamine (Paneco), 100 units/ml of penicillin, and 100 µg/ml of streptomycin (Paneco) at 37 °C in ambient atmosphere with 5% CO_2. The cells were cultured in 25-cm^2 flasks (SPL Life Sciences) and re-seeded using 0.25% trypsin in Versene solution (Paneco). For experiments, HeLa cells were seeded on 35-mm confocal dishes (SPL Life Sciences, #100350) with glass bottoms (diameter 13 mm) at a density of 30,000 cells/ml in 2 ml of culture medium. The day after seeding, culture medium was removed, and the cells were washed from residual medium with 2 ml of Hanks' balanced salt solution (HBSS). After removal of HBSS, 200 µl of a previously isolated serum sample was added into the hole of a confocal dish to fully cover the cells grown on the glass bottom. Serum samples were pre-warmed to 37 °C before addition to the cultured cells. After addition of sera, confocal dishes were incubated for 30 min at 37 °C in ambient atmosphere with 5% CO_2. Then, cells were washed twice with 2 ml of HBSS and fixed with 4% paraformaldehyde in PBS (pH 7.4) for 20 min at room temperature (RT). Similarly, four additional control dishes with HeLa cells were treated with a thymidine analogue (BrdU, IdU, CldU, or EdU) dissolved in HBSS to a final concentration of 10 µM.

Detection of BrdU, IdU, and CldU by immunofluorescence staining

For a given experiment, a series of slices from each mouse was transferred into a well of a 24-well plate. The slices were treated with 2 N HCl for 40 min at 37 °C for the DNA denaturation necessary for antigen unmasking. Shrunken slices were recovered by incubation in 1 M borate (Sigma-Aldrich, #B6768) for 10 min at RT with an exchange. All remaining procedures were conducted at RT. After three washes in PBS, slices were permeabilized in 2% Triton X-100 (Sigma-Aldrich, #T8787) in PBS for 1 h followed by blocking in 10% goat serum (Sigma-Aldrich, #G9023) in PBS containing 0.2% Triton X-100 for 1 h. Then, slices from mice injected with BrdU or CldU were stained with rat anti-BrdU antibody clone BU1/75 (Abcam, #ab6326) at a dilution of 1:1000, whereas slices from mice injected with IdU were stained with mouse anti-BrdU antibody clone B44 (BD Biosciences, #347580) at a dilution of 1:1000. Clone BU1/75 exhibits strong affinity to both BrdU and CldU, whereas clone B44 exhibits high affinity to IdU with slightly weaker affinity to BrdU (Aten et al. 1992; Manders et al. 1992; Vega and Peterson 2005; Liboska et al. 2012). After three washes in PBS, the slices were stained with goat anti-rat IgG antibody conjugated with Alexa488 (Thermo Fisher Scientific, #A-11006) at a dilution of 1:500 or goat anti-mouse IgG antibody conjugated with Alexa488 (Thermo Fisher Scientific, #A-11029) at a dilution of 1:500. Primary and secondary antibodies were diluted in 5% goat serum in PBS containing 0.2% Triton X-100. Slices were incubated in the primary antibodies overnight and in the secondary antibodies for 2 h at RT with slight rocking. Stained slices were washed three times in PBS, attached to gelatin-coated glass slides, mounted in VECTASHIELD® Antifade Mounting Medium (Vector Laboratories, #H-1000-10), and coverslipped.

The cells treated with sera or pure thymidine analogues were exposed to 2 N HCl for 15 min at 37 °C followed by permeabilization in 0.5% Triton X-100 in PBS for 30 min and blocking in 10% goat serum in PBS containing 0.1% Triton X-100 for 30 min. Then, the cells were incubated in the same primary and secondary antibodies diluted in 5% goat serum in PBS containing 0.1% Triton X-100 for 4 h and 2 h, respectively. To stain nuclei, the fluorescent dye DAPI (Sigma-Aldrich, #D9542) was added to the secondary antibody solution to a final concentration of 2 µg/ml. The stained cells were mounted in VECTASHIELD® Antifade Mounting Medium.

Detection of EdU by click reaction

Series of slices from mice that received EdU and cells treated with EdU-containing sera were permeabilized in 2% Triton

X-100 in PBS for 1 h and in 0.5% Triton X-100 in PBS for 30 min, respectively. After three washes in PBS, both slices and cells were exposed to a click reaction for 15 min at RT with slight rocking. The composition of the click reaction was 20 mM (+)-sodium L-ascorbate (Sigma-Aldrich, #A4034), 10 µM Alexa 488-azide (Thermo Fisher Scientific, #A10266), and 4 mM copper sulfate (Sigma-Aldrich, #C1297) in PBS. Stained slices were washed three times in PBS, attached to gelatin-coated glass slides, mounted in VECTASHIELD® Antifade Mounting Medium, and coverslipped. The cells were additionally stained for 30 min with the fluorescent dye DAPI dissolved in PBS at a final concentration of 2 µg/ml and mounted in VECTASHIELD® Antifade Mounting Medium.

Cell counting on brain slices

For determination of labeling kinetics in vivo, cells in the subgranular zone of the hippocampal DG that incorporated thymidine analogues were manually counted using a Nikon ECLIPSE Ti2-E epi-fluorescence microscope equipped with a 40X objective (numerical aperture 0.95). Cell counting was blinded. On each slice in a particular series, we identified the subgranular zone between the granular layer and hilus using the differential interference contrast (DIC) mode of the microscope. In each field of view, we focused on the uppermost surface of a slice using the DIC mode of the microscope, and, then, we switched to the fluorescence mode to visualize labeled cell nuclei. By moving the focus drive, individual labeled cell nuclei were identified and counted on a given field of view. Here, we considered labeled cell nuclei within the uppermost focal plane as the boundary-touching objects and, therefore, excluded them from counting. By repeating this procedure, we counted labeled cell nuclei throughout the DG subgranular zone identified in a particular slice. Cell counts obtained for all slices of a given series were summed and then extrapolated to the entire hippocampal DG of both hemispheres by multiplication by 12 (6 wells per hemisphere and 2 hemispheres per brain).

Microscopy

Cell preparations were captured using a Nikon ECLIPSE Ti2-E epi-fluorescent microscope equipped with a SPECTRA X light engine and a Teledyne Photometrics BSI camera. DAPI and Alexa488 were excited by solid-state light sources with wavelengths of 395 nm and 470 nm, respectively. Images were acquired using Nikon NIS-Elements software. The light source intensity and camera settings were initially adjusted for the cells treated with sera collected 10 min after pulse label delivery. Then, the same light source intensity and camera settings were employed for both the cells treated with sera and the control cells treated only with modified nucleotides. Five randomly selected fields of view were captured for each cell preparation using a 20X objective (numerical aperture 0.75).

Determination of labeling indices and mean fluorescence intensities in cells treated with sera

Quantification of labeled nuclei and measurements of mean fluorescence intensities on images obtained from cell culture samples treated with sera and pure thymidine analogues were performed using ImageJ software (National Institutes of Health, Bethesda, MD, USA). To determine the numbers of labeled nuclei (stained for BrdU, IdU, CldU, or EdU) and total numbers of nuclei (stained with DAPI) on images, we applied the Threshold function with default settings to identify the edges of objects and convert the original images into binary images. Then, the Watershed function was used to separate adjacent nuclei followed by counting of the determined objects using the command Analyze particles. To exclude small objects, minimal object space was set as 60 μm^2. Labeling indices for individual images were determined as the ratio of the labeled nuclei number to total nuclei number. A labeling index for an individual cell culture sample was calculated by averaging the labeling indices determined for five images. Labeling indices of individual cell culture samples were used to build resultant graphs and to perform statistical analysis. To measure mean fluorescence intensities, we used the Threshold function with default settings to identify the edges of objects on a duplicated image. Then, regions of interest (ROIs) were selected using the Create Selection function, saved to the ROI manager, and applied to the original image. The Measure function was applied to determine mean fluorescence intensities for all identified ROIs. The mean fluorescence intensity for an individual image was calculated by averaging mean fluorescence intensities determined for all ROIs. Similarly, the mean fluorescence intensity for an individual cell culture sample was calculated by averaging mean fluorescence intensities determined for five images. The mean fluorescence intensities of individual cell culture samples were normalized to an average of fluorescence intensities determined for samples treated with sera collected at the 10 min time point. The relative fluorescence intensities of individual cell culture samples were used to build resultant graphs and to perform statistical analysis.

Data analysis

All quantitative data were expressed as mean ± standard error the of mean (SEM) and subjected to statistical analysis using the Kruskal–Wallis test with Dunn's post hoc test. Differences between the means of experimental groups with p values below 0.05 were considered significant.

Results

Labeling kinetics of BrdU, IdU, CldU, and EdU in vivo

To determine the labeling kinetics of BrdU, IdU, CldU, and EdU in vivo, we quantified labeled cell nuclei in the hippocampal DG of adult mice and determined how their number depends on the time interval after intraperitoneal injection of a given label. The DG is a brain area where stem and progenitor cells continuously divide to generate new granular neurons throughout adulthood (Kuhn et al. 1996; van Praag et al. 2002). Among other brain regions where cells have been reported to proliferate, the DG is particularly suitable for the quantitative analysis of labeling kinetics for several reasons. First, the DG is a spatially confined structure. This enables extrapolation of cell counts determined with a limited series of sections to the entire DG (Encinas and Enikolopov 2008). Second, dividing cells of the DG do not form tight clusters and, therefore, can be more easily discriminated and counted than, for instance, in the subventricular zone (SVZ). Third, the population of dividing cells in the DG is asynchronous, i.e., cells are randomly distributed through cell-cycle phases, and it is homogenous in terms of the S-phase and cell-cycle lengths (Nowakowski et al. 1989; Hayes and Nowakowski 2002; Encinas et al. 2011; Podgorny et al. 2018). In other words, dividing cells in the DG represent a proliferative population with known cell-cycle kinetics. When a nucleotide label is delivered intraperitoneally, it diffuses into the blood circulation system, rapidly disperses throughout the organism, and, when reaching the DG, is incorporated into the newly replicating DNA of cells passing the S-phase at that moment. Since dividing cells in the DG are progressing through the cell cycle, a cohort of labeled cells soon exits the S-phase, whereas an equal number of unlabeled cells passing the late G1-phase enter the S-phase, becoming labeled. Therefore, the number of labeled cells should gradually increase while the label is available. When the label is depleted via its incorporation into the synthesized strands of DNA and metabolization, the labeling of cells that enter the S-phase de novo ceases, and the number of labeled cells remains unchanged before they reach mitosis. Taking into account reports that indicate that the G2/M phase of dividing DG cells is longer than 4 h (Fischer et al. 2014), we collected brains for analysis at the time points 10, 20, 30, 60, 120, or 240 min after pulse label delivery.

Counting of labeled cell nuclei on the series of brain slices revealed that for all tested modified nucleotides, their number rises with the lengthening of the time interval between pulse label delivery and sample collection and reaches a plateau at 60 min (Fig. 2). Labeled cell numbers at 10 min were ~ 65–85% of the plateau levels. These observations indicate that a vast majority of proliferating cells in the DG incorporate each of tested labels at a detectable level within 10 min of injection and that no notable increase in labeled nuclei number occurs after 60 min. Our experiments also indicate that all modified nucleotides tested in our study exhibit similar labeling kinetics in vivo.

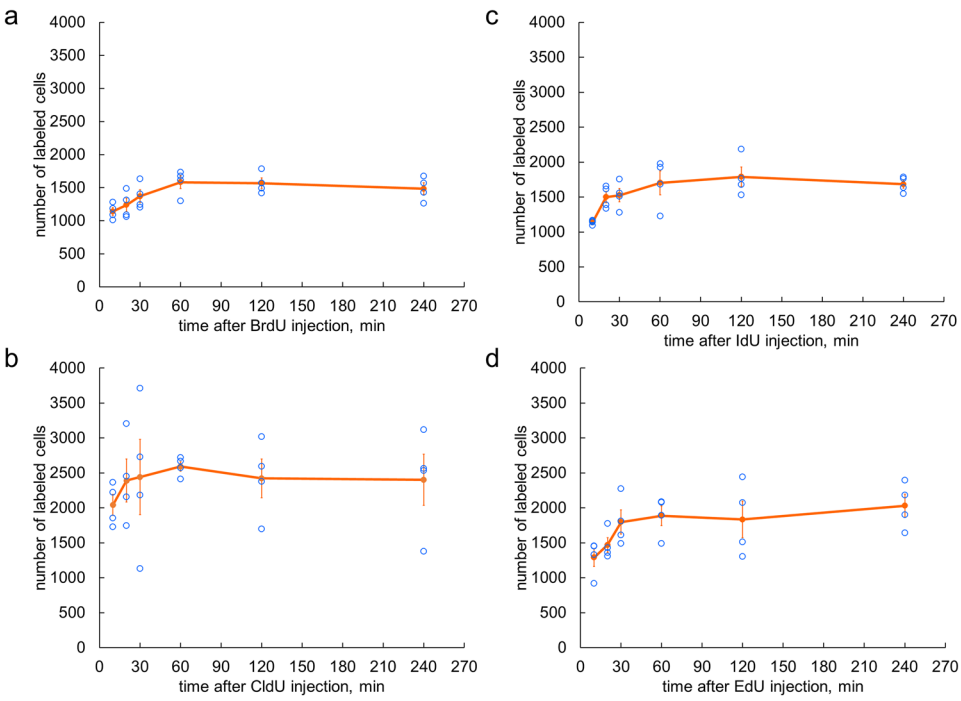

Fig. 2 Labeling kinetics of thymidine analogues. Labeled cell number in the DG was quantified 10, 20, 30, 60, 120, and 240 min after a single intraperitoneal administration of BrdU (**a**), IdU (**b**), CldU (**c**), or EdU (**d**). Data are presented as mean ± SEM. Differences between time points are not statistically significant (Kruskal–Wallis test with Dunn's post hoc test, $n = 4$ for each time point)

Clearance of BrdU, IdU, CldU, and EdU from blood serum

We next asked whether the cessation of label incorporation into the replicating DNA reflects an overall depletion of the label in the blood. For that, we determined the time intervals during which BrdU, IdU, CldU, and EdU are still present in the blood serum in amounts sufficient to label cells grown in culture, at levels detectable by our immunohistochemical staining and click reaction procedures. We collected the blood sera from the same mice that were used for the analysis of labeling kinetics in vivo, added the blood sera to cultivated HeLa cells, and 30 min later determined the cell labeling indices, with another HeLa cell sample treated with 10 μM of the corresponding label serving as a reference (Fig. 3a). Blood sera obtained from animals 10, 20, 30, and 60 min after the injection of BrdU, CldU, or EdU, when added to HeLa cells, induced identical labeling indices of ~ 50% for each time point (Fig. 3b, d, e). No labeled cells were detected in HeLa cell samples treated with blood sera derived from mice 120 and 240 min after nucleotide injection.

A similar analysis of HeLa cell samples treated with blood sera from animals injected with IdU revealed similar labeling indices at the time points 10, 20, 30, 60, and 120 min, with no labeled cells detected with blood sera derived at the 240 min time point (Fig. 3c). For each modified nucleotide, the labeling indices, where they differed from zero, were equal to the reference labeling indices determined for the nucleotides directly added to HeLa cells. These observations indicate that BrdU, CldU, and EdU remain in the blood serum at concentrations sufficient to label cells at detectable levels at least within 60 min of the pulse delivery of the label, with IdU exhibiting a longer presence in the blood serum. Interestingly, in each case when HeLa cells incorporated the label, we did not observe a decline in labeling indices as a function of increased time interval between the label delivery to the animal and blood serum collection.

Therefore, we next examined whether gradual clearance of a given label from the blood serum is reflected in changes in mean fluorescence intensities of the labeled HeLa cell nuclei. To this end, we determined mean fluorescence intensities for individual labeled HeLa cell nuclei treated with blood sera and then averaged these measurements for each time point. Since all images within an individual series of cell culture samples were captured under the same illumination and detection conditions, we normalized the averaged intensities of each cell culture sample for a resultant mean intensity calculated for the samples treated with sera collected 10 min after pulse label delivery. Analysis of relative fluorescence intensities in cell cultures exposed to blood sera containing BrdU, IdU, or CldU did not show any notable changes in detected signals as a function of the time interval between the pulse label delivery and blood collection (Fig. 4a–c). Unlike halogenated thymidine analogues, the intensity of the EdU signal decreased along with the increase of the time interval between the pulse label delivery and blood collection, with a statistically significant difference in the EdU signal between the 20 and 60 min time points (Fig. 4d). These observations suggest that labeling signal in cell nuclei of cell culture samples treated with sera containing halogenated thymidine analogues does not correlate with true label content in the blood sera. At the same time, the observed decline in the EdU signal may reflect gradual clearance of the label from blood serum after a pulse label delivery.

Discussion

Here, we evaluated the bioavailability time of the most frequently used thymidine analogues by examining the labeling kinetics for BrdU, IdU, CldU, and EdU in vivo after a single intraperitoneal injection as well as their availability in the blood serum of the injected animals. Our results indicate that all the tested thymidine analogues exhibit similar cell labeling kinetics and are cleared from the blood circulation system within almost equal time intervals. The characteristic times of label incorporation into replicating DNA of dividing cells in vivo and label availability in blood serum are confined to 1 h, with longer availability of IdU in blood serum (2 h). The current study combined with our earlier evidence on triple-S-phase labeling (Podgorny et al. 2018) validates the labeling equivalency of all tested thymidine analogues if they are used at equimolar doses. Our findings are important for the practical use of the most broadly employed thymidine analogues. They also ensure the consistency of labeling results when conducting single-, double-, or triple-S-phase labeling in vivo using BrdU, IdU, CldU, and EdU in various combinations and orders.

Our observations on the labeling kinetics of BrdU and its clearance from blood serum indicate that BrdU bioavailability time is limited to 1 h, with the bulk of label incorporation occurring within the first 10–30 min and no significant increase in the number of labeled cells in vivo 1 h after label injection. These observations are in a good agreement with previously reported estimates of BrdU bioavailability time determined by a variety of detection methods, primarily via evaluation of label uptake into replicating DNA and label clearance from blood serum (Packard et al. 1973; Barker et al. 2013; Matiašová et al. 2014). However, some studies report shorter bioavailability times of 30 min (Hayes and Nowakowski 2000) or even 15 min (Mandyam et al. 2007). The differences in the bioavailability time estimates may originate primarily from the specimen types used and methods employed. Unlike other studies, here, we employ two

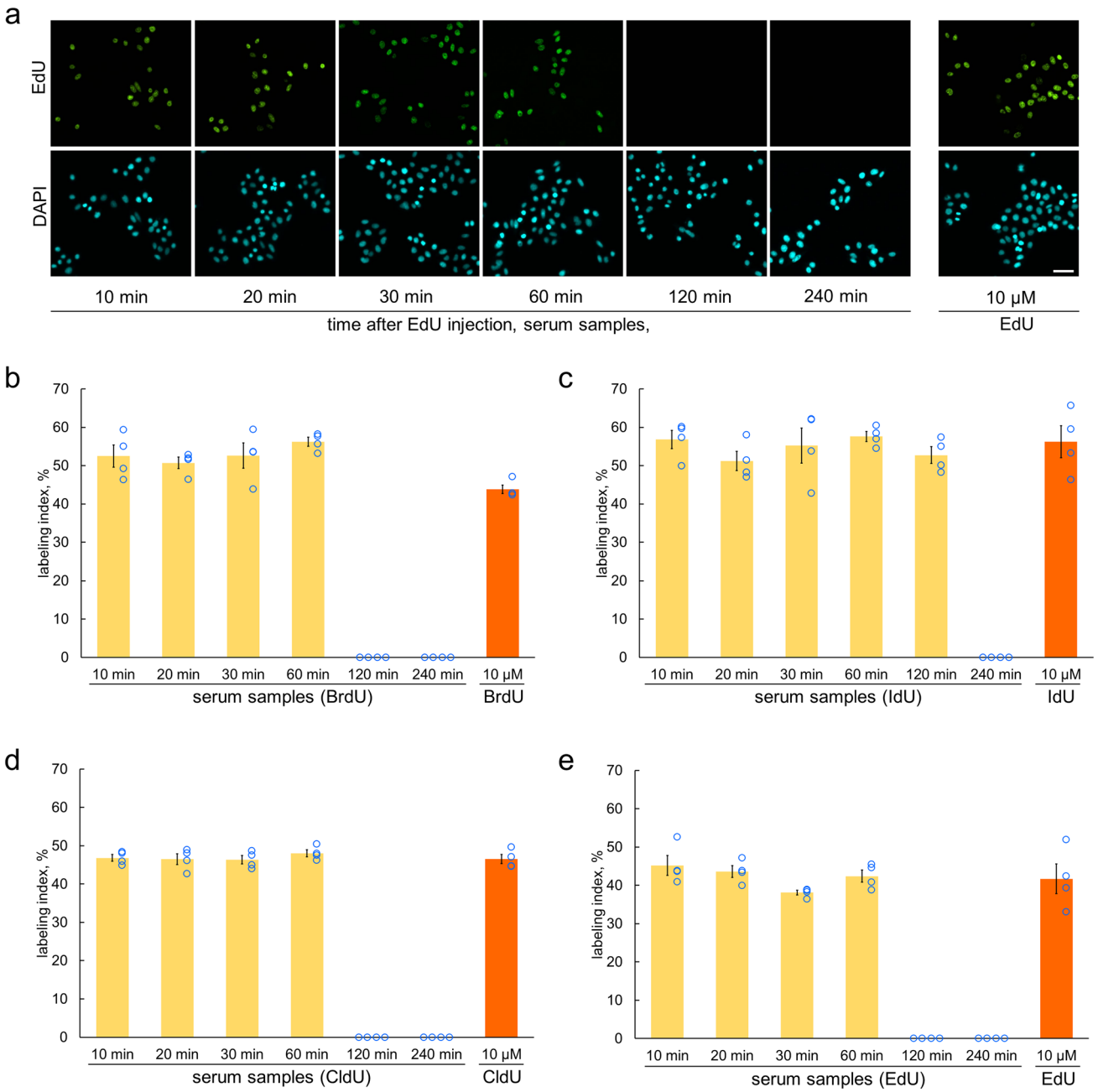

Fig. 3 Determination of label clearance from blood serum using cell culture assay. Following a single intraperitoneal administration of nucleotides, blood serum samples were collected 10, 20, 30, 60, 120, and 240 min after the injection. Representative images of HeLa cells after a 30 min treatment with blood sera collected from mice that received a single intraperitoneal injection of EdU or a 30 min treatment with 10 µM EdU (**a**). Labeling indices for BrdU (**b**), IdU (**c**), CldU (**d**), and EdU (**e**). Labeling indices were determined as percentages of labeled cell numbers (label-positive nuclei) to total cell number (DAPI-positive nuclei). HeLa cells treated with pure thymidine analogues at a concentration 10 µM served as reference samples for revealing the S-phase cohort. Quantitative data are presented as mean ± SEM. Differences between time points are not statistically significant (Kruskal–Wallis test with Dunn's post hoc test, $n = 4$ for each time point). Scale bar: 50 µm

methods: (i) quantitative analysis of labeled cell numbers in the hippocampal DG of the mouse brain at different time points after pulse label delivery and (ii) cell culture assay for the presence of available nucleotides in the blood sera collected from the same animals. Both methods are indirect (they rely on counting of labeled cells detected by immunohistochemistry or click reaction). Therefore, they are not sensitive enough to perform rigorous quantitative analysis of label incorporation and clearance. However, these methods enable determining time points when the amount of an

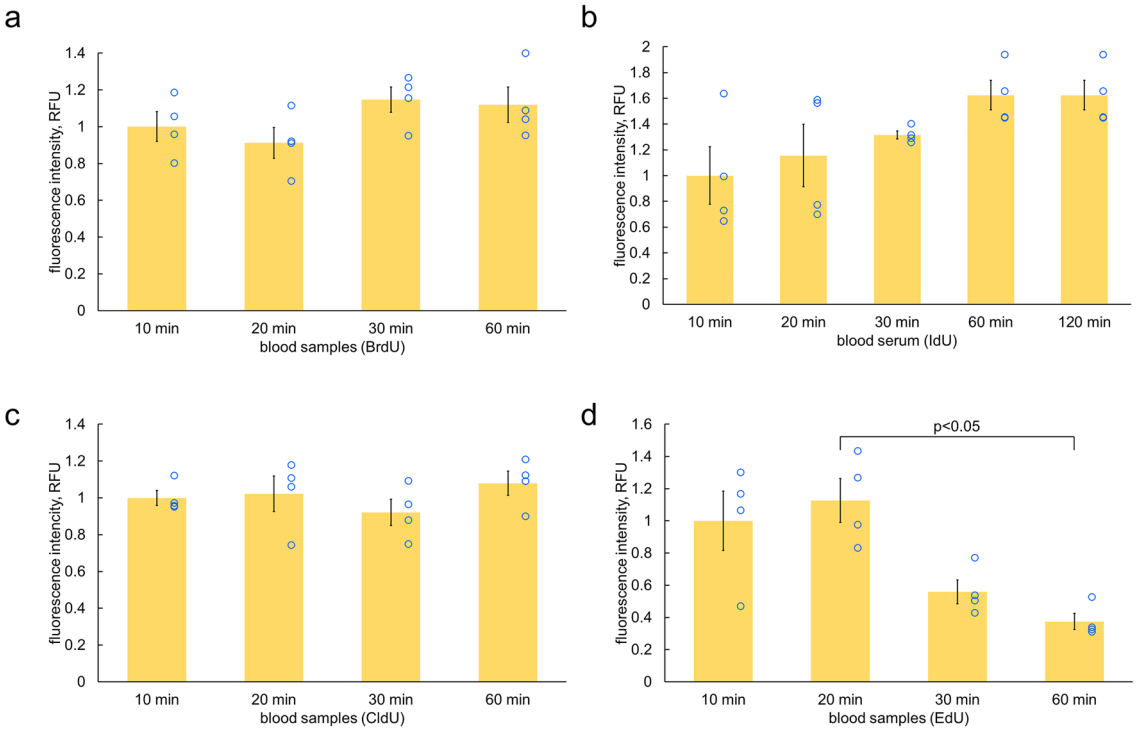

Fig. 4 Determination of mean signal intensities in labeled nuclei of HeLa cells treated with blood sera collected from mice at different time points after pulse label delivery. BrdU (**a**), IdU (**b**), CldU (**c**), or EdU (**d**). Mean fluorescence intensity was determined for each labeled nucleus followed by averaging for all labeled cells for an individual cell culture sample. Next, mean fluorescence intensities of individual cell culture samples were normalized to the average fluorescence intensity determined for 10 min cell culture samples. Resultant signal intensities are expressed in relative fluorescence units (RFU). Quantitative data are presented as mean ± SEM. Statistical analysis was performed using the Kruskal–Wallis test with Dunn's post hoc test, $n = 4$ for each time point

available thymidine analogue in the brain tissue and blood serum decreases to levels at which the labeling of cells passing the S-phase is no longer detectable by immunohistochemistry or click reaction. Combining experimental data obtained by both methods allows us to estimate the bioavailability time at accuracy enough for the practical use of the examined thymidine analogues. Experimental evidence for BrdU availability and clearance obtained by both methods is consistent and is in agreement with previous findings. We consider this as an important validation of our estimates of the labeling and clearance kinetics for IdU, CldU, and EdU.

Analysis of labeling kinetics in vivo revealed that all examined labels mark the bulk of dividing cells (approximately 65–85% of the cell numbers at the plateau level) within first 10 min of pulse label delivery. This observation is in line with previous evidence that, within the first 15 min, BrdU labels approximately 85% of the S-phase cohort that can be detected at 2 h (Mandyam et al. 2007). Similarities in relative labeling levels and kinetics at early time points after pulse label delivery between the examined thymidine analogues enables quantitative analysis of dividing cells over short periods of time. This option is useful for certain experimental schemes. In other cases, when precise evaluations are necessary, collection of specimens should be performed more than 1 h after the pulse label delivery to exclude underestimation of the labeled cell number.

Analysis of labeling in vivo also revealed that the number of labeled cells at the plateau varied between cohorts of animals receiving individual modified nucleotides. Previous studies showed that BrdU, IdU, CldU, and EdU mark equal numbers of cells when intraperitoneally injected at equimolar doses into the same animal for double- or triple-S-phase labeling (Zeng et al. 2010; Podgorny et al. 2018). Therefore, we speculate that observed differences are related to variability in age composition of animal cohorts used for studying individual modified nucleotides rather than to distinctions in labeling ability or detection methods of individual modified nucleotides delivered at equimolar doses.

Our cell culture assay for studying the clearance of the thymidine analogues from the blood serum after pulse label delivery showed that BrdU, CldU, and EdU are present in blood serum in amounts sufficient for marking cultured cells at detectable levels for least 1 h after the nucleotides were injected into the animals, with the IdU being available for labeling even 2 h after the nucleotide injection. The longer presence of IdU in blood serum in

comparison to other thymidine analogues is potentially related to the higher injection volumes used. However, this does not contribute to labeling kinetics in vivo, which is indistinguishable from the kinetics determined for the other thymidine analogues. Our estimate of the clearance time for BrdU is higher than the estimates obtained in other studies which employed a similar cell culture assay in combination with immunohistochemical or flow cytometric determination of labeled cells (Barker et al. 2013; Matiašová et al. 2014). In these studies, sera from BrdU-injected animals exhibited either undetectable or low labeling levels at 1 h. These slight differences may be due to the variances in the doses of BrdU delivered: 150 mg/kg in the present study, 100 mg/kg in Barker et al. (2013), and 50 mg/kg in Matiašová et al. (2014). We used the 150 mg/kg BrdU dose in our study because it was previously determined as the saturating dose which excludes the underestimation of cell cohorts in the S-phase (Mandyam et al. 2007). BrdU doses near saturation were found to provide consistent quantitative data (Burns and Kuan 2005), and in most experimental situations, BrdU doses ranging from 50 to 100 mg/kg produce an appropriate labeling level. Hence, our estimates of the bioavailability time for BrdU are also valid for those experimental situations where lower doses of BrdU are used. Similarly, we speculate that the same consideration is valid for the other thymidine analogues examined in our study.

Interestingly, we did not observe notable changes in labeling indices at all time points where they were not equal to zero. Moreover, the labeling indices obtained for serum samples were equal to those of control cells treated with individual modified nucleotides. A decline of the labeling index in relation to the time interval between pulse label delivery and blood sample collection could be expected because the nucleotide label is gradually cleared from the bloodstream and its concentration in blood serum decreases with time (Packard et al. 1973; Stetson et al. 1985; Phuphanich and Levin 1985). Lower amounts of the label in serum would be expected to produce incomplete labeling of the S-phase cohort. However, in our study, we did not observe a decline in labeling indices. In previous studies (Barker et al. 2013; Matiašová et al. 2014), incomplete labeling of the S-phase cohort with BrdU was observed for at least one examined time point. This dissimilarity can be explained by the differences in sensitivities of the methods and antibody clones used for detecting BrdU in our and other studies. Yet another explanation may be that in our study, the time intervals where label amount in the blood sera decreases so that incomplete labeling of the S-phase cohort occurs did not overlap with the time points analyzed in those studies. Hence, our data on labeling indices do not allow us to evaluate the dynamics of label clearance from blood serum. We, therefore, assessed mean fluorescence intensities of labeled nuclei to ask whether changes in fluorescence signals can reveal the label clearance dynamics. Similar to labeling indices, we did not observe any notable changes in fluorescence signals of labeled nuclei for the halogenated thymidine analogues BrdU, IdU, and CldU at all time points where labeled HeLa cells were detected. However, the EdU signal declined with increase of the time intervals between pulse label delivery and serum collection. These observations can be explained by the following. The halogenated thymidine analogues are detected by indirect immunofluorescence staining in which secondary antibodies are polyclonal and carry variable numbers of fluorochromes. Therefore, the relationship between the number of antigen–first antibody interactions and the resultant number of fluorochromes is not proportional. In contrast, EdU is detected by the covalent binding of a fluorescent azide to the ethynyl group via click reaction (Salic and Mitchison 2008). Unlike halogenated thymidine analogues, the relationship between the number of EdU molecules and the number of bound fluorochromes is strictly proportional. Our observations suggest that the examined labels remain at a saturated concentration that provides robust labeling of dividing cells in the cell culture assay in terms of labeling indices and signal levels in labeled nuclei at all tested time points.

In sum, our results indicate that the thymidine analogues BrdU, IdU, CldU, and EdU, that are most frequently used for marking dividing cells in vivo, exhibit similar labeling kinetics and clearance rates after a single intraperitoneal injection to mice. Their bioavailability time is, on average, 1 h with a slightly increased value for IdU. Our findings are of practical significance for designing labeling schemes and for the interpretation of labeling readouts when performing double- or triple-S-phase labeling in vivo using various combinations and orders of BrdU, IdU, CldU, and EdU.

Funding This study was funded by the Russian Foundation for Basic Research, grant no. 19-29-04016 (to O.V.P.), the Ministry of Science and Higher Education of the Russian Federation grant no. 075-15-2019-1789 to the Center for Precision Genome Editing and Genetic Technologies for Biomedicine (to O.V.P.), NIH (NIA grant AG057705 to G.E.), and Russian Science Foundation, grant no. 19-15-00247 (to G.E.).

Availability of data and material Not applicable.

Code availability Not applicable.

Declarations

Conflict of interest The authors declare no conflict of interest.

Ethics approval All experiments on mice were performed according to European Convention for the Protection of Vertebrate Animals

used for Experimental and other Scientific Purposes (1986, ETS 123) and approved by the Institutional Animal Care and Use Committee of Shemyakin-Ovchinnikov Institute of Bioorganic Chemistry (protocol no. 281).

References

Alexiades MR, Cepko C (1996) Quantitative analysis of proliferation and cell cycle length during development of the rat retina. Dev Dyn 205:293–307. https://doi.org/10.1002/(SICI)1097-0177(199603)205:3%3c293::AID-AJA9%3e3.0.CO;2-D

Angevine JB, Sidman RL (1961) Autoradiographic study of cell migration during histogenesis of cerebral cortex in the mouse. Nature 192:766–768. https://doi.org/10.1038/192766b0

Aten JA, Bakker PJ, Stap J et al (1992) DNA double labelling with IdUrd and CldUrd for spatial and temporal analysis of cell proliferation and DNA replication. Histochem J 24:251–259. https://doi.org/10.1007/bf01046839

Barker JM, Charlier TD, Ball GF, Balthazart J (2013) A new method for in vitro detection of bromodeoxyuridine in serum: a proof of concept in a songbird species, the canary. PLoS One 8:e63692. https://doi.org/10.1371/journal.pone.0063692

Brandt MD, Hübner M, Storch A (2012) Brief report: adult hippocampal precursor cells shorten S-phase and total cell cycle length during neuronal differentiation. STEM CELLS 30:2843–2847. https://doi.org/10.1002/stem.1244

Burns KA, Kuan C-Y (2005) Low doses of bromo- and iododeoxyuridine produce near-saturation labeling of adult proliferative populations in the dentate gyrus. Eur J Neurosci 21:803–807. https://doi.org/10.1111/j.1460-9568.2005.03907.x

Cai L, Hayes NL, Nowakowski RS (1997) Local homogeneity of cell cycle length in developing mouse cortex. J Neurosci 17:2079–2087

Encinas JM, Enikolopov G (2008) Identifying and quantitating neural stem and progenitor cells in the adult brain. Methods in cell biology. Elsevier, Amsterdam, pp 243–272

Encinas JM, Michurina TV, Peunova N et al (2011) Division-coupled astrocytic differentiation and age-related depletion of neural stem cells in the adult hippocampus. Cell Stem Cell 8:566–579. https://doi.org/10.1016/j.stem.2011.03.010

Fischer TJ, Walker TL, Overall RW et al (2014) Acute effects of wheel running on adult hippocampal precursor cells in mice are not caused by changes in cell cycle length or S phase length. Front Neurosci. https://doi.org/10.3389/fnins.2014.00314

Gratzner HG (1982) Monoclonal antibody to 5-bromo- and 5-iododeoxyuridine: a new reagent for detection of DNA replication. Science 218:474–475. https://doi.org/10.1126/science.7123245

Hayes NL, Nowakowski RS (2000) Exploiting the dynamics of S-phase tracers in developing brain: interkinetic nuclear migration for cells entering versus leaving the S-phase. Dev Neurosci 22:44–55. https://doi.org/10.1159/000017426

Hayes NL, Nowakowski RS (2002) Dynamics of cell proliferation in the adult dentate gyrus of two inbred strains of mice. Dev Brain Res 134:77–85. https://doi.org/10.1016/S0165-3806(01)00324-8

Kriss JP, Revesz L (1962) The distribution and fate of bromodeoxyuridine and bromodeoxycytidine in the mouse and rat. Cancer Res 22:254–265

Kuhn H, Dickinson-Anson H, Gage F (1996) Neurogenesis in the dentate gyrus of the adult rat: age-related decrease of neuronal progenitor proliferation. J Neurosci 16:2027–2033. https://doi.org/10.1523/JNEUROSCI.16-06-02027.1996

Liboska R, Ligasová A, Strunin D et al (2012) Most anti-BrdU antibodies react with 2'-deoxy-5-ethynyluridine—the method for the effective suppression of this cross-reactivity. PLoS One 7:e51679. https://doi.org/10.1371/journal.pone.0051679

Ma H, Samarabandu J, Devdhar RS et al (1998) Spatial and temporal dynamics of DNA replication sites in mammalian cells. J Cell Biol 143:1415–1425. https://doi.org/10.1083/jcb.143.6.1415

Manders EM, Stap J, Brakenhoff GJ et al (1992) Dynamics of three-dimensional replication patterns during the S-phase, analysed by double labelling of DNA and confocal microscopy. J Cell Sci 103(Pt 3):857–862

Manders EMM, Stap J, Strackee J et al (1996) Dynamic behavior of DNA replication domains. Exp Cell Res 226:328–335. https://doi.org/10.1006/excr.1996.0233

Mandyam CD, Harburg GC, Eisch AJ (2007) Determination of key aspects of precursor cell proliferation, cell cycle length and kinetics in the adult mouse subgranular zone. Neuroscience 146:108–122. https://doi.org/10.1016/j.neuroscience.2006.12.064

Matiašová A, Ševc J, Mikeš J et al (2014) Flow cytometric determination of 5-bromo-2′-deoxyuridine pharmacokinetics in blood serum after intraperitoneal administration to rats and mice. Histochem Cell Biol 142:703–712. https://doi.org/10.1007/s00418-014-1253-7

Neef AB, Luedtke NW (2011) Dynamic metabolic labeling of DNA in vivo with arabinosyl nucleosides. Proc Natl Acad Sci USA 108:20404–20409. https://doi.org/10.1073/pnas.1101126108

Neef AB, Luedtke NW (2014) An azide-modified nucleoside for metabolic labeling of DNA. ChemBioChem 15:789–793. https://doi.org/10.1002/cbic.201400037

Newton PT, Li L, Zhou B et al (2019) A radical switch in clonality reveals a stem cell niche in the epiphyseal growth plate. Nature 567:234–238. https://doi.org/10.1038/s41586-019-0989-6

Nowakowski RS, Rakic P (1974) Clearance rate of exogenous 3H-thymidine from the plasma of pregnant rhesus monkeys. Cell Tissue Kinet 7:189–194. https://doi.org/10.1111/j.1365-2184.1974.tb00411.x

Nowakowski RS, Lewin SB, Miller MW (1989) Bromodeoxyuridine immunohistochemical determination of the lengths of the cell cycle and the DNA-synthetic phase for an anatomically defined population. J Neurocytol 18:311–318. https://doi.org/10.1007/bf01190834

Packard DS, Menzies RA, Skalko RG (1973) Incorportaiton of thymidine and its analogue, bromodeoxyuridine, into embryos and maternal tissues of the mouse. Differentiation 1:397–404. https://doi.org/10.1111/j.1432-0436.1973.tb00137.x

Phuphanich S, Levin VA (1985) Bioavailability of bromodeoxyuridine in dogs and toxicity in rats. Cancer Res 45:2387–2389

Podgorny O, Peunova N, Park J-H, Enikolopov G (2018) Triple S-phase labeling of dividing stem cells. Stem Cell Rep 10:615–626. https://doi.org/10.1016/j.stemcr.2017.12.020

Rieder U, Luedtke NW (2014) Alkene-tetrazine ligation for imaging cellular DNA. Angew Chem Int Ed Engl 53:9168–9172. https://doi.org/10.1002/anie.201403580

Rubini JR, Cronkite EP, Bond VP, Fliedner TM (1960) The metabolism and fate of tritiated thymidine in man. J Clin Invest 39:909–918. https://doi.org/10.1172/JCI104111

Saffhill R, Hume WJ (1986) The degradation of 5-iododeoxyuridine and 5-bromodeoxyuridine by serum from different sources and its consequences for the use of the compounds for incorporation into DNA. Chem Biol Interact 57:347–355. https://doi.org/10.1016/0009-2797(86)90008-6

Salic A, Mitchison TJ (2008) A chemical method for fast and sensitive detection of DNA synthesis in vivo. Proc Natl Acad Sci USA 105:2415–2420. https://doi.org/10.1073/pnas.0712168105

Schweyer K, Rüschoff-Steiner C, Arias-Carrión O et al (2019) Neuronal precursor cells with dopaminergic commitment in the rostral migratory stream of the mouse. Sci Rep 9:13359. https://doi.org/10.1038/s41598-019-49920-5

Staroscik RN, Jenkins WH, Mendelsohn ML (1964) Availability of tritiated thymidine after intravenous administration. Nature 202:456–458. https://doi.org/10.1038/202456a0

Steinhauser ML, Bailey AP, Senyo SE et al (2012) Multi-isotope imaging mass spectrometry quantifies stem cell division and metabolism. Nature 481:516–519. https://doi.org/10.1038/nature10734

Stetson PL, Shukla UA, Amin PR, Ensminger WD (1985) High-performance liquid chromatographic method for the determination of bromodeoxyuridine and its major metabolite, bromouracil, in biological fluids. J Chromatogr B Biomed Sci Appl 341:217–222. https://doi.org/10.1016/S0378-4347(00)84032-3

Takahashi T, Nowakowski RS, Caviness VS (1993) Cell cycle parameters and patterns of nuclear movement in the neocortical proliferative zone of the fetal mouse. J Neurosci 13:820–833

Takahashi T, Nowakowski RS, Caviness VS (1994) Mode of cell proliferation in the developing mouse neocortex. Proc Natl Acad Sci USA 91:375–379. https://doi.org/10.1073/pnas.91.1.375

Taylor JH, Woods PS, Hughes WL (1957) The organization and duplication of chromosomes as revealed by autoradiographic studies using tritium-labeled thymidine. Proc Natl Acad Sci USA 43:122–128. https://doi.org/10.1073/pnas.43.1.122

van Praag H, Schinder AF, Christie BR et al (2002) Functional neurogenesis in the adult hippocampus. Nature 415:1030–1034. https://doi.org/10.1038/4151030a

Vega CJ, Peterson DA (2005) Stem cell proliferative history in tissue revealed by temporal halogenated thymidine analog discrimination. Nat Methods 2:167–169. https://doi.org/10.1038/nmeth741

Verdoodt F, Willems M, Mouton S et al (2012) Stem cells propagate their DNA by random segregation in the flatworm Macrostomum lignano. PLoS One 7:e30227. https://doi.org/10.1371/journal.pone.0030227

Zeng C, Pan F, Jones LA et al (2010) Evaluation of 5-ethynyl-2'-deoxyuridine staining as a sensitive and reliable method for studying cell proliferation in the adult nervous system. Brain Res 1319:21–32. https://doi.org/10.1016/j.brainres.2009.12.092

Publisher's Note Springer Nature remains neutral with regard to jurisdictional claims in published maps and institutional affiliations.